The Deubiquitinase USP36 Regulates Growth and Spermatogenesis Through Catalytic-Dependent and -Independent Mechanisms in *Drosophila*

Carmen Coirry[1], Julie Manessier[1], Charlène Clot[1, #a], Magda Mortier[1], Marie-Odile Fauvarque[1] and Emmanuel Taillebourg[1, *]

1 Univ. Grenoble Alpes, CEA, INSERM, BGE U1038, F-38000 Grenoble, France

#a Current Address: Institut de Génétique Moléculaire de Montpellier, Univ Montpellier, CNRS, Montpellier, France

* Corresponding author
E-mail: emmanuel.taillebourg@cea.fr

Running title: Catalytic-Dependent and -Independent functions of USP36

Keywords: DUB, MYC, CRISPR/Cas9, cell growth, spermatogenesis

ABSTRACT

Deubiquitinases (DUBs) form a specific class of proteases removing ubiquitin from target proteins. They are involved in the regulation of many cellular processes including cell growth and proliferation. Among them, USP36 is a key regulator of the oncogenic transcription factor c-Myc, preventing its degradation by the proteasome. These two proteins form an evolutionary conserved complex providing the opportunity to investigate USP36 mechanisms of action *in vivo* in a genetically tractable model such as *Drosophila melanogaster*. Null mutants of *dUsp36* die early during larval development and exhibit severe growth defects. Strikingly, we report here that flies carrying a CRISPR/Cas9-induced catalytic mutation of *dUsp36* survive to adulthood with only minor growth defects, yet males are infertile. This finding indicates that dUSP36 deubiquitinating activity is dispensable for cell growth but essential for spermatogenesis. Our results thus reveal that dUSP36 functions through both catalytic-dependent and catalytic-independent mechanisms, highlighting a dual mode of action with implications for the understanding of DUBs mechanism of action.

INTRODUCTION

Deubiquitinases (DUBs) are proteases that specifically remove ubiquitin moieties from ubiquitinated proteins (KOMANDER *et al.* 2009; CLAGUE *et al.* 2013). They regulate numerous cellular processes, including protein stability, cell signalling and endocytosis (CLAGUE *et al.* 2012; LEZNICKI AND KULATHU 2017). Their dysregulation has been linked to numerous human cancers, underlining the importance of understanding their mechanisms of action (SACCO *et al.* 2010; FRAILE *et al.* 2012; DEWSON *et al.* 2023). In particular, USP36, a DUB primarily localized in the nucleolus, is overexpressed in various human cancers, including subsets of breast, lung, and ovarian cancers (LI *et al.* 2008; LUO *et al.* 2024; NIU *et al.* 2024; XU *et al.* 2024). It has been shown to support ribosomal biogenesis and maintain nucleolar integrity by deubiquitinating and stabilizing multiple nucleolar proteins, such as c-MYC, DHX33, SNAIL1, and RNA Pol I, thereby protecting them from proteasomal degradation (ENDO *et al.* 2009a; ENDO *et al.* 2009b; SUN *et al.* 2015a; FRAILE *et al.* 2018; VAN DEN HEUVEL *et al.* 2021; QIN *et al.* 2023; YANG *et al.* 2024). The role of USP36 in nucleolar c-MYC regulation has been

extensively studied (SUN *et al.* 2015a; SUN *et al.* 2015b; LIU *et al.* 2019; THEVENON *et al.* 2020; HU AND LUO 2024), as tight control of c-MYC levels is essential for normal cell growth and proliferation, while its dysregulation drives cancer development (VAN RIGGELEN *et al.* 2010; MILLER *et al.* 2012). c-MYC regulates the expression of thousands of genes, coordinating key cellular processes, including ribosome biogenesis, RNA transcription, and protein synthesis (SABO AND AMATI 2014; GRIFONI AND BELLOSTA 2015). RNAi-mediated knockdown of USP36 significantly reduces nucleolar c-MYC levels and decreases cell proliferation (SUN *et al.* 2015a). It remains unclear whether this phenotype arises from USP36 depletion or whether its enzymatic activity is also involved.

We previously showed that in the model organism *Drosophila melanogaster*, the *dUsp36* gene encodes multiple isoforms, one of which localizes to the nucleolus, is required for cell and organismal growth, and stabilizes dMYC (THEVENON *et al.* 2020). To further investigate the *in vivo* mechanisms of action of dUSP36 and the specific role of its DUB activity, we generated a catalytically inactive version of the endogenous dUSP36 protein using CRISPR/Cas9 mutagenesis. Here, we demonstrate that unlike *dUsp36* null mutants, which completely lack dUSP36 protein and exhibit severe growth defects leading to larval lethality, *dUsp36* catalytic mutants display only minor growth defects and develop to adulthood. Interestingly, *dUsp36* catalytic mutant males display a strongly reduced fertility correlated with low sperm production. Altogether, these findings reveal that while the presence of the dUSP36 protein is essential for cellular and organismal growth, its catalytic activity is not. However, it is critically required for spermatogenesis. These results demonstrate that*, in vivo*, dUSP36 functions through both catalytic-dependent and catalytic-independent mechanisms, revealing a dual mode of action.

RESULTS

Generation of *dUsp36* catalytic mutants by CRISPR/Cas9 mutagenesis

To generate a catalytically inactive version of the dUSP36 protein, we mutated the cysteine residue (C181) within a conserved domain previously shown to be essential for the DUB activity of other ubiquitin-specific proteases (HU *et al.* 2005; KOMANDER *et al.* 2009; FAESEN *et al.* 2011; YE *et al.* 2011) to a serine residue using CRISPR/Cas9 mediated mutagenesis (Fig. S1A; see Materials and Methods for details). This C181S mutation had been previously

shown to completely abolish dUSP36 catalytic activity (BUSZCZAK *et al.* 2009). The CRISPR/Cas9 mutagenesis process identified two independent *dUsp36*^{C181S} mutant strains, as well as a control strain, *dUsp36*^{CTL}, which contains the same silent mutations introduced for screening purposes as the mutant alleles, but not the G-to-C transversion encoding the C181S mutation (Fig. S1C).

Western blot analysis of dUSP36 expression reveals that the dUSP36^{C181S} protein is detected at lower levels than the wild-type dUSP36 protein, whereas the *dUsp36*^{CTL} allele produces normal dUSP36 protein levels (Fig. 1A, B). This observation aligns with previous findings showing that dUSP36 undergoes auto-deubiquitination to regulate its stability – a function that the mutated form is unable to fulfil (THEVENON *et al.* 2020). To ensure comparable dUSP36 protein levels across genotypes, we thus compared *dUsp36*^{C181S} mutants to *dUsp36*^{CTL}/*dUsp36*$^{\Delta 43}$ heterozygous controls (Fig. 1B). Importantly, the subcellular localization of the dUSP36^{C181S} protein is indistinguishable from that of the wild-type dUSP36 protein (Fig. 1C). These data confirm the successful generation of the catalytically inactive dUsp36^{C181S} mutant allele, which provide a valuable tool for investigating the specific role of dUSP36 catalytic activity in vivo.

dUsp36 catalytic mutants are viable and exhibit a subtle growth phenotype

We previously reported that *dUsp36*$^{\Delta 43}$ null mutants, which completely lack dUSP36 protein, exhibit severe growth defects and early larval lethality (TAILLEBOURG *et al.* 2012). In addition, *dUsp36*^{D1} hypomorphic mutants, which fail to express the main dUSP36 isoform, display reduced growth rate, developmental delay, and a strong decrease in adult body weight (THEVENON *et al.* 2020). These observations clearly establish that the presence of dUSP36 protein is required for cellular and organismal growth. In sharp contrast with these previous observations, we found that *dUsp36*^{C181S} mutant flies develop to adulthood without displaying developmental lethality (Fig 3B) and exhibit only a minor reduction in body weight compared to heterozygous controls (Fig. 2A, B), along with a slight decrease in wing size (Fig. 2C, D).

The enzymatic activity of USPs relies on a catalytic triad—a conserved set of three key amino acid residues consisting of a cysteine, a histidine, and an aspartate or asparagine. As mentioned previously, cysteine-to-serine mutations are typically used to abolish DUB activity; however, histidine-to-aspartate mutations have also been reported to render the

enzyme catalytically inactive (KOVALENKO *et al.* 2003; HU *et al.* 2005; KOMANDER *et al.* 2009). To confirm our observation, we mutated both the cysteine and histidine residues and generated transgenic flies expressing the dUSP36$^{C181S, H439D}$ protein. When ubiquitously expressed in a *dUsp36* null mutant background, this double mutant protein rescues the larval lethality of *dUsp36* null mutants and allows for the emergence of viable adults (Fig. S2). These results confirm that the catalytic activity of dUSP36 is not essential for cellular growth and organismal viability.

To determine whether the observed phenotypes result from cell-autonomous factors, we generated clones of larval fat body cells homozygous for either the control allele *dUsp36*^{CTL}, the catalytically inactive allele *dUsp36*^{C181S}, the hypomorphic allele *dUsp36*^{D1}, or the null allele *dUsp36*$^{\Delta 43}$ (Fig. 2E). Clonal analysis revealed that *dUsp36*^{C181S} mutant cells are significantly smaller than neighbouring wild-type cells, although their growth is much less affected than that of hypomorphic or null *dUsp36* mutant cells (Fig. 2F). This observation indicates that the subtle growth defect of *dUsp36* catalytic mutants is cell-autonomous. Altogether, these results demonstrate that while the presence of dUSP36 protein is essential for cellular and organismal growth, its catalytic activity plays only a minor, cell-autonomous role in this process.

Altering dMYC protein levels in *dUsp36* catalytic mutants

Experimental data obtained in human cellular models (KOVALENKO *et al.* 2003; HU *et al.* 2005; KOMANDER *et al.* 2009) provide compelling evidence that USP36 depletion affects the stability of nucleolar c-MYC and inhibit cell proliferation. To test whether the minor growth defects of *dUsp36* catalytic mutants depend on dMYC function, we evaluated the phenotypic consequences of altered dMYC protein levels in *dUsp36* wild-type or mutant contexts.

To increase dMYC levels, we introduced a transgene expressing a GFP-tagged version of dMYC within its genomic environment providing additional *dMyc* copies alongside the wild-type *dMyc* locus (GREER *et al.* 2013). In contrast to what is observed with strong dMYC overexpression, this transgene does not induce cell death, and fully rescues the lethality of *dMyc*^{4} null mutants, demonstrating that it expresses physiological levels of functional dMYC protein (data not shown, (GREER *et al.* 2013)). Remarkably, when introduced into either control, hypomorphic, or catalytically inactive *dUsp36* mutant backgrounds, this transgene significantly enhances the body weight of both control and *dUsp36* hypomorphic mutant

flies but not that of *dUsp36* catalytic mutants (Fig. 3A). These results indicate that while control and hypomorphic *dUsp36* mutant flies respond to dMYC overexpression—suggesting that reduced dMYC protein levels contribute to the growth defects of *dUsp36* hypomorphic mutants—*dUsp36* catalytic mutants do not.

To further explore the genetic interaction between dMyc and dUSP36, we used the $dMyc^{P0}$ hypomorphic mutation that decreases dMYC protein levels and leads to a reduced body weight (JOHNSTON *et al.* 1999). *dUsp36* catalytic mutants and $dMyc^{P0}$ mutants develop to adulthood without developmental lethality (Fig. 3B). In contrast, in a $dMyc^{P0}$ genetic background, the frequency of $dUsp36^{C181S}$ mutants is significantly reduced (Fig. 3B), whereas no such reduction of viability is observed in *dUsp36* control flies. This implies that while dUSP36 catalytic activity is dispensable under normal conditions, it becomes critical when *dMyc* function is compromised.

To determine whether these findings hold true at the organ level, we compared the effects of altered dMYC protein levels in the developing wing between control flies and *dUsp36* catalytic mutants (Fig. 3C). In this setup, wing-specific increase of dMYC protein levels were achieved by reducing AGO protein levels using wing-directed expression of a specific RNAi transgene silencing *Ago* expression. Indeed, AGO is the F-box component of the SCF E3 ligase complex which ubiquitinates dMYC and negatively regulates dMYC protein levels *in vivo* (MOBERG *et al.* 2004). Knocking down *Ago* leads to elevated dMYC protein levels and increased tissue growth (MOBERG *et al.* 2004) without causing the deleterious effects associated with strong dMYC overexpression (GREER *et al.* 2013). As expected, in control flies, reducing AGO protein levels results in increased wing area (Fig. 3C). In contrast, reducing AGO levels in the developing wing of *dUsp36* catalytic mutants does not significantly increase wing size (Fig. 3C). These results indicate that increased dMYC levels promote wing growth in control flies but not in *dUsp36* catalytic mutant flies.

Reciprocally, dMYC protein levels were then specifically reduced by expressing a *dMyc* targeting RNAi transgene in the developing wing. In that context, both control flies and *dUsp36* catalytic mutants displayed reduced wing size (Fig. 3C). Two-way ANOVA analysis reveals that *dUsp36* catalytic mutants are more affected by dMYC depletion than control flies (Fig. 3D).

Altogether these results show that, at both the organismal and organ levels, increased dMYC levels fail to increase body weight or wing area in *dUsp36* catalytic mutants, whereas they do

in control and *dUsp36* hypomorphic backgrounds. This suggests that reduced dMYC protein levels are not the primary cause of the growth defect of *dUsp36* catalytic mutants. In contrast, *dUsp36* catalytic mutants exhibit a strong sensitivity to dMYC depletion, suggesting that, *in vivo*, dUSP36 catalytic activity acts in the same pathway as dMYC to promote growth.

***dUsp36* catalytic mutation affects male fertility**

Specific combinations of viable *dUsp36* loss-of-function alleles have been shown to affect male and female fertility (BUSZCZAK *et al.* 2009). We observed here that *dUsp36*^{C181S} females are slightly but significantly less fertile than control females (Fig. 4A). It remains unclear however whether this decreased fertility is due to a general effect related to their reduced body weight or a specific role of dUSP36 catalytic activity in female gametogenesis. Strikingly, *dUsp36* catalytic mutant males produce significantly fewer offspring than control males, with most being completely sterile (Fig. 4B). Consistent with this observation, *dUsp36*^{C181S} males exhibit reduced seminal vesicle size, indicating lower sperm production compared to control males. Moreover, we show here that dUSP36 protein is widely expressed during spermatogenesis (Fig. 4C, D). These findings reveal that dUSP36 catalytic activity plays a critical role in spermatogenesis.

DISCUSSION

The data presented here demonstrate that inactivating the catalytic activity of the DUB USP36 in *Drosophila* is not equivalent to its complete or partial depletion. In particular, the catalytic mutant does not display the cell and organismal growth defects observed in null or hypomorphic *dUsp36* mutant. This indicates that dUSP36 functions primarily through non-catalytic mechanisms in these processes. In contrast we report that USP36 DUB activity is essential for male fertility, making it the only process identified so far that strictly depends upon USP36 enzymatic function.

It is unlikely that the *dUsp36*^{C181S} mutation fails to fully inhibit the DUB activity *in vivo* contrary to expectations from the literature. Indeed, the lower protein levels of dUSP36C^{181S} compared to wild-type dUSP36 (Fig. 1A, B) indicate that it fails to stabilizes itself, unlike the wild-type form, which undergoes auto-deubiquitination, strongly suggesting that this protein

is indeed catalytically inactive (THEVENON *et al.* 2020). Furthermore, a double-mutant dUSP36 protein, in which both the catalytic cysteine and the histidine residue of the conserved catalytic triad are mutated, is still able to sustain cell and organismal growth in a null mutant background *in vivo*. These results strongly argue against the hypothesis that the minor growth defect observed in dUsp36^{C181S} mutants is due to residual DUB activity.

We further showed that *dUsp36* catalytic mutants do not respond to increased dMYC levels, whereas wild-type and *dUsp36* hypomorphic mutants do. This suggests that reduced dMYC levels do not contribute to the minor growth defects observed in *dUsp36^{C181S}* mutants. However, these mutants are highly sensitive to dMYC depletion, indicating that dUSP36 catalytic activity likely plays a role in the same pathway as dMYC. Taken together, our results indicate that dUSP36 primarily functions independently of its enzymatic activity in promoting cell growth and that – in contrast to previous conclusions based on silencing or overexpressing experiments - its catalytic activity is not required for dMYC stabilization in vivo.

These results should be considered in the context of existing literature, including our own work, showing that in *Drosophila* and human cultured cells, USP36 deubiquitinates and stabilizes MYC (SUN *et al.* 2015a; SUN *et al.* 2015b; THEVENON *et al.* 2020). Several hypotheses could explain this discrepancy: (1) The deubiquitination and stabilization of MYC by USP36 observed in cultured cells may also occur *in vivo* but could be compensated by redundant regulatory mechanisms. If this is the case, USP36 would be expected to regulate another dMYC-independent growth process through a non-catalytic mechanism. In this line, recent studies in human cells indicate that USP36 functions as a SUMO ligase to promote the SUMOylation of specific nucleolar proteins involved in ribosome biogenesis, a process crucially required for promoting cell and organism growth (RYU *et al.* 2021; CHEN *et al.* 2023; LI *et al.* 2023; LI *et al.* 2024; YANG *et al.* 2024). Moreover, in human cells, the catalytic cysteine of USP36 is essential for both its DUB and SUMO ligase activities (RYU *et al.* 2021). If Drosophila dUSP36 functions similarly as its human orthologue, *dUsp36^{C181S}* mutants should also lack SUMO ligase activity, which would impair ribosome biogenesis and induce severe growth defects as observed in Minute mutants (REF). However, the mild growth phenotype of *dUsp36^{C181S}* mutants does not support this hypothesis. Additionally, we failed to detect SUMO ligase activity for dUSP36 in *Drosophila* cells (data not shown). (2) Contrary to previous conclusions based on knock-down experiments, USP36 may control MYC stability

independently from its catalytic activity: it may not directly deubiquitinate MYC but instead regulate its ubiquitination level indirectly. This could occur through inhibition of an E3 ligase targeting MYC or recruitment of another DUB within the regulatory complex. In this model, USP36 knock-down via RNAi or loss-of-function mutations would impair these functions, leading to MYC destabilization. Moreover, overexpressing wild-type USP36 may result in non-specific deubiquitination of MYC, whereas a catalytically inactive USP36 mutant would not act ectopically, falsely leading to the conclusion that USP36 directly deubiquitinates MYC (SUN *et al.* 2015a; THEVENON *et al.* 2020). Additional experiments will be needed to clarify the exact mechanisms by which USP36 regulates MYC and contributes to cell growth.

While dUSP36 catalytic activity plays a minor role in cell and organismal growth, our results clearly demonstrate that it is essential for spermatogenesis. This is consistent with previous findings showing that dUSP36 is required for germline stem cell maintenance by deubiquitinating histone H2B and repressing premature expression of differentiation genes (BUSZCZAK *et al.* 2009).

In conclusion, our findings indicate that, in *Drosophila*, dUSP36 functions through a dual mechanism: in cell growth, dUSP36 acts independently of its catalytic activity, similar to other DUBs or pseudo-DUBs (CAMPOS ALONSO AND KNOBELOCH 2024) whereas in spermatogenesis, its DUB activity is crucial, highlighting a specialized catalytic function in germline development. Our results therefore reshape the way mechanisms of action of DUBs are considered during cell response and development, extending beyond their enzymatic activity. Determining whether this dual mechanism is unique to dUSP36 or extends to its human counterpart and other DUBs will be of great interest.

MATERIALS AND METHODS

Drosophila strains

The null, *dUsp36*$^{\Delta 43}$, and hypomorphic, *dUsp36*^{D1} alleles and the *UAS-dUsp36*$^{C181S,\ H439D}$ transgenic line have already been described (THEVENON *et al.* 2009; TAILLEBOURG *et al.* 2012; THEVENON *et al.* 2020).

The Bloomington Drosophila Stock Center provided the following Drosophila strains: *Tg dMyc* (#81274), *dMyc*^{P0} (#11298), *UAS-dMyc-IR* (# 25783), *UAS-Ago-IR* (#34802), *nubGal4* (#25754), *hsFLP* (#8862), *FRT2A Gal80* (#5190), *FRT2A* (#1997) and *CgGal4* (#7011).

CRISPR/Cas9 mutagenesis

The gRNA sequence was selected using the E-CRISP website (http://www.e-crisp.org/) and cloned into the pCFD3 plasmid (PORT *et al.* 2014). A 169-nucleotide long single stranded oligonucleotide donor (ssODN) repair template was synthesised (https://eu.idtdna.com/page). It contains the mutation of interest, as well as silent mutations of the Protospacer Adjacent Motif (PAM) and of the gRNA to avoid re-cleaving of an edited chromosome. In addition, the nucleotide sequence close to the desired site of modification was modified by introduction of a silent mutation, in order to create a Pst1 restriction site (Sup. Fig. 1A). The ssODN was injected along with the sgRNA expression vector (ssODN: 100 ng/uL and sgRNA: 250 ng/uL) into the nos-Cas9 (PORT *et al.* 2014) recipient strain (BestGene Inc.). Sixty-six F0 founders were crossed individually and up to 10 F1 males were crossed individually for each F0 founder; after 4-5 days in the crossing vials, each F1 male was retrieved for single fly DNA extraction. After amplification, PCR products were digested by Pst1, leading to the identification of six independent Pst1 positive strains (Sup. Fig. 1B). Sequencing revealed that three of them contained the desired C181S mutation (two, *dUsp36*$^{C181S-1}$ and *dUsp36*$^{C181S-2}$, were kept for further analysis) whereas three others did not include the C181S mutation but contains all the silent mutations (Sup. Fig. 1C). One of them, *dUsp36*^{CTL}, was used as control.

To ensure that the mutagenesis process did not add any off-target mutations, the genomic region was sequenced and these alleles were outcrossed for six generations on a wild-type chromosome. Moreover, all the phenotypic analyses were performed on heterozygotes (*dUsp36*^{CTL}/*dUsp36*$^{\Delta 43}$ and *dUsp36*$^{C181S-1}$/*dUsp36*$^{C181S-2}$).

Western blots

Protein lysates were separated on SDS-PAGE gels (TGX Stain Free from BioRad). Proteins were transferred to PVDF membranes (BioRad). Membranes were saturated for 1h in PBS/0.1% Tween-20/5% BSA or skimmed milk, incubated with the appropriate primary antibody for 1 to 3h at RT or overnight at 4°C in PBS/0.1% Tween-20/1% BSA or skimmed

milk before 3 washes in TBS/0.1% Tween-20 (PBST) and then incubated an additional hour at RT with corresponding secondary antibodies coupled to horse radish peroxidase (HRP). After 3 rinses with PBST, the membranes were revealed with the Luminata Forte Western HRP substrate (Millipore) using the Chemidoc imaging system (BioRad). Quantifications were performed using the Image Lab software (BioRad). The anti-dUSP36 antibody, a kind gift from Dr. M. Buszczak, was used at a 1/2500 dilution

Immunohistochemistry

Lateral lobes of third instar larval fat bodies or adult testes were dissected in PBS, fixed for 30 min in 4% paraformaldehyde and rinsed twice in PBS. The samples were then blocked for 1 h in PBS, 0.1% Triton X-100, 5% normal goat serum and incubated overnight at 4°C with the anti-dUSP36 (1/200) and anti-Fibrillarin 38F3 (1/200, abcam) antibodies. Secondary antibodies were coupled to Alexa594 or Alexa488 (1/500, Invitrogen). After mounting in DAPI containing Vectashield (Vector Laboratories, H-1200), the samples were imaged using a Zeiss LSM 880 confocal laser scanning microscope.

Phenotypic analysis

For weight measurements, the larval density was carefully controlled. Three-day-old females were weighted by groups of ten on a Mettler Toledo Classic precision balance. Adults and dissected wings were imaged using a Keyence VHX-5000 numerical microscope. Wing areas were blindly measured manually using the Fiji/ImageJ software (National Institute of Health). For clonal analysis of cell size in the fat body, 0–6 h embryos were subjected to heat-shock for 1 h at 37°C and resulting 4.5 days old L3 larvae were dissected. Fat body's lateral lobes were fixed for 30 min in 4% paraformaldehyde, rinsed twice in PBS, and incubated overnight at 4°C in 2 U/ml Alexa Fluor 546 Phalloidin (Invitrogen, A22283). After mounting in DAPI containing Vectashield (Vector Laboratories, H-1200), the samples were imaged using a Zeiss LSM 880 confocal laser scanning microscope. Cell size was quantified using the Fiji/ImageJ software (National Institute of Health) as the ratio between the area of a GFP+ cell and the mean area of neighbouring GFP- cells.

For the fertility tests, female and male flies of the indicated genotype were collected and aged for 3 days. They were then individually mated to three Canton-S flies of the opposite sex. The vials were emptied after a three-day period and the progeny was counted.

All the statistical analyses were performed using the GraphPad Prism6 software.

AKNOWLEDGEMENT

We are particularly indebted to Dr. M. Buszczak for the anti-dUSP36 antibody and to the Bloomington *Drosophila* Stock Center (BDSC) (NIH P40OD018537) for providing *Drosophila* strains. Confocal microscopy was performed at the µLife facility of the Interdisciplinary Research Institute of Grenoble (IRIG).
This work was supported by the French National Research Agency in the framework of the "Investissements d'avenir" program (ANR-17-EURE-0003) through a funding from GRAL, the Grenoble Alliance for Integrated Structural and Cell Biology. Thesis operating costs are supported by IDEX Université Grenoble Alpes (IRGA2024 –MUTE – G7H-IRG24E80) and GRAL PhD Operating Costs (CC).

REFERENCES

Buszczak, M., S. Paterno and A. C. Spradling, 2009 Drosophila stem cells share a common requirement for the histone H2B ubiquitin protease scrawny. Science 323: 248-251.

Campos Alonso, M., and K. P. Knobeloch, 2024 In the moonlight: non-catalytic functions of ubiquitin and ubiquitin-like proteases. Front Mol Biosci 11: 1349509.

Chen, Y., Y. Li, R. S. Dai, J. C. Savage, U. Shinde *et al.*, 2023 The ubiquitin-specific protease USP36 SUMOylates EXOSC10 and promotes the nucleolar RNA exosome function in rRNA processing. Nucleic Acids Res 51: 3934-3949.

Clague, M. J., I. Barsukov, J. M. Coulson, H. Liu, D. J. Rigden *et al.*, 2013 Deubiquitylases from genes to organism. Physiol Rev 93: 1289-1315.

Clague, M. J., J. M. Coulson and S. Urbe, 2012 Cellular functions of the DUBs. J Cell Sci 125: 277-286.

Dewson, G., P. J. A. Eichhorn and D. Komander, 2023 Deubiquitinases in cancer. Nat Rev Cancer 23: 842-862.

Endo, A., N. Kitamura and M. Komada, 2009a Nucleophosmin/B23 regulates ubiquitin dynamics in nucleoli by recruiting deubiquitylating enzyme USP36. J Biol Chem 284: 27918-27923.

Endo, A., M. Matsumoto, T. Inada, A. Yamamoto, K. I. Nakayama *et al.*, 2009b Nucleolar structure and function are regulated by the deubiquitylating enzyme USP36. J Cell Sci 122: 678-686.

Faesen, A. C., M. P. Luna-Vargas, P. P. Geurink, M. Clerici, R. Merkx *et al.*, 2011 The differential modulation of USP activity by internal regulatory domains, interactors and eight ubiquitin chain types. Chem Biol 18: 1550-1561.

Fraile, J. M., D. Campos-Iglesias, F. Rodriguez, A. Astudillo, R. Vilarrasa-Blasi *et al.*, 2018 Loss of the deubiquitinase USP36 destabilizes the RNA helicase DHX33 and causes preimplantation lethality in mice. J Biol Chem 293: 2183-2194.

Fraile, J. M., V. Quesada, D. Rodriguez, J. M. Freije and C. Lopez-Otin, 2012 Deubiquitinases in cancer: new functions and therapeutic options. Oncogene 31: 2373-2388.

Greer, C., M. Lee, M. Westerhof, B. Milholland, R. Spokony *et al.*, 2013 Myc-dependent genome instability and lifespan in Drosophila. PLoS One 8: e74641.

Grifoni, D., and P. Bellosta, 2015 Drosophila Myc: A master regulator of cellular performance. Biochim Biophys Acta 1849**:** 570-581.

Hu, M., P. Li, L. Song, P. D. Jeffrey, T. A. Chenova *et al.*, 2005 Structure and mechanisms of the proteasome-associated deubiquitinating enzyme USP14. EMBO J 24**:** 3747-3756.

Hu, Y., and M. Luo, 2024 Cinobufotalin regulates the USP36/c-Myc axis to suppress malignant phenotypes of colon cancer cells in vitro and in vivo. Aging (Albany NY) 16**:** 5526-5544.

Johnston, L. A., D. A. Prober, B. A. Edgar, R. N. Eisenman and P. Gallant, 1999 Drosophila myc regulates cellular growth during development. Cell 98**:** 779-790.

Komander, D., M. J. Clague and S. Urbe, 2009 Breaking the chains: structure and function of the deubiquitinases. Nat Rev Mol Cell Biol 10**:** 550-563.

Kovalenko, A., C. Chable-Bessia, G. Cantarella, A. Israel, D. Wallach *et al.*, 2003 The tumour suppressor CYLD negatively regulates NF-kappaB signalling by deubiquitination. Nature 424**:** 801-805.

Leznicki, P., and Y. Kulathu, 2017 Mechanisms of regulation and diversification of deubiquitylating enzyme function. J Cell Sci 130**:** 1997-2006.

Li, J., L. M. Olson, Z. Zhang, L. Li, M. Bidder *et al.*, 2008 Differential display identifies overexpression of the USP36 gene, encoding a deubiquitinating enzyme, in ovarian cancer. Int J Med Sci 5**:** 133-142.

Li, Y., T. S. Carey, C. H. Feng, H. M. Zhu, X. X. Sun *et al.*, 2023 The Ubiquitin-specific Protease USP36 Associates with the Microprocessor Complex and Regulates miRNA Biogenesis by SUMOylating DGCR8. Cancer Res Commun 3**:** 459-470.

Li, Y., Y. Yang, R. C. Sears, M. S. Dai and X. X. Sun, 2024 USP36 SUMOylates Las1L and Promotes Its Function in Pre-Ribosomal RNA ITS2 Processing. Cancer Res Commun 4**:** 2835-2845.

Liu, Q., W. Sheng, Y. Ma, J. Zhen, S. Roy *et al.*, 2019 USP36 protects proximal tubule cells from ischemic injury by stabilizing c-Myc and SOD2. Biochem Biophys Res Commun 513**:** 502-508.

Luo, L., Y. Li, R. Huang, L. Li, C. Wu *et al.*, 2024 USP36 plays an oncogenic role in colorectal cancer cells. Neoplasma 71**:** 13-21.

Miller, D. M., S. D. Thomas, A. Islam, D. Muench and K. Sedoris, 2012 c-Myc and cancer metabolism. Clin Cancer Res 18**:** 5546-5553.

Moberg, K. H., A. Mukherjee, A. Veraksa, S. Artavanis-Tsakonas and I. K. Hariharan, 2004 The Drosophila F box protein archipelago regulates dMyc protein levels in vivo. Curr Biol 14**:** 965-974.

Niu, M. Y., Y. J. Liu, J. J. Shi, R. Y. Chen, S. Zhang *et al.*, 2024 The Emerging Role of Ubiquitin-Specific Protease 36 (USP36) in Cancer and Beyond. Biomolecules 14.

Port, F., H. M. Chen, T. Lee and S. L. Bullock, 2014 Optimized CRISPR/Cas tools for efficient germline and somatic genome engineering in Drosophila. Proc Natl Acad Sci U S A 111**:** E2967-2976.

Qin, K., S. Yu, Y. Liu, R. Guo, S. Guo *et al.*, 2023 USP36 stabilizes nucleolar Snail1 to promote ribosome biogenesis and cancer cell survival upon ribotoxic stress. Nat Commun 14**:** 6473.

Ryu, H., X. X. Sun, Y. Chen, Y. Li, X. Wang *et al.*, 2021 The deubiquitinase USP36 promotes snoRNP group SUMOylation and is essential for ribosome biogenesis. EMBO Rep 22**:** e50684.

Sabo, A., and B. Amati, 2014 Genome recognition by MYC. Cold Spring Harb Perspect Med 4.

Sacco, J. J., J. M. Coulson, M. J. Clague and S. Urbe, 2010 Emerging roles of deubiquitinases in cancer-associated pathways. IUBMB Life 62**:** 140-157.

Sun, X. X., X. He, L. Yin, M. Komada, R. C. Sears *et al.*, 2015a The nucleolar ubiquitin-specific protease USP36 deubiquitinates and stabilizes c-Myc. Proc Natl Acad Sci U S A 112**:** 3734-3739.

Sun, X. X., R. C. Sears and M. S. Dai, 2015b Deubiquitinating c-Myc: USP36 steps up in the nucleolus. Cell Cycle 14**:** 3786-3793.

Taillebourg, E., I. Gregoire, P. Viargues, A. C. Jacomin, D. Thevenon *et al.*, 2012 The deubiquitinating enzyme USP36 controls selective autophagy activation by ubiquitinated proteins. Autophagy 8**:** 767-779.

Thevenon, D., E. Engel, A. Avet-Rochex, M. Gottar, E. Bergeret *et al.*, 2009 The Drosophila ubiquitin-specific protease dUSP36/Scny targets IMD to prevent constitutive immune signaling. Cell Host Microbe 6**:** 309-320.

Thevenon, D., I. Seffouh, C. Pillet, X. Crespo-Yanez, M. O. Fauvarque *et al.*, 2020 A Nucleolar Isoform of the Drosophila Ubiquitin Specific Protease dUSP36 Regulates MYC-Dependent Cell Growth. Front Cell Dev Biol 8**:** 506.

van den Heuvel, J., C. Ashiono, L. C. Gillet, K. Dorner, E. Wyler *et al.*, 2021 Processing of the ribosomal ubiquitin-like fusion protein FUBI-eS30/FAU is required for 40S maturation and depends on USP36. Elife 10.

van Riggelen, J., A. Yetil and D. W. Felsher, 2010 MYC as a regulator of ribosome biogenesis and protein synthesis. Nat Rev Cancer 10**:** 301-309.

Xu, H., T. Wang, H. Nie, Q. Sun, C. Jin *et al.*, 2024 USP36 promotes colorectal cancer progression through inhibition of p53 signaling pathway via stabilizing RBM28. Oncogene 43**:** 3442-3455.

Yang, Y., Y. Li, R. C. Sears, X. X. Sun and M. S. Dai, 2024 SUMOylation regulation of ribosome biogenesis: Emerging roles for USP36. Front RNA Res 2.

Ye, Y., M. Akutsu, F. Reyes-Turcu, R. I. Enchev, K. D. Wilkinson *et al.*, 2011 Polyubiquitin binding and cross-reactivity in the USP domain deubiquitinase USP21. EMBO Rep 12**:** 350-357.

FIGURE LEGENDS

Figure 1

Expression of the dUSP36^{C181S} protein. (A) Total protein extracts from *Drosophila* males of the indicated genotypes were analysed by Western blot using a specific anti-dUSP36 antibody. (B) Quantification of dUSP36 relative levels, expressed as the ratio of dUSP36 signal intensity to Actin signal intensity, normalized to the wild-type Canton-S strain. N = 4. ** indicates a statistically significant difference ($P < 0.01$) as determined by one-way ANOVA. (C) Fat bodies of third-instar larvae stained with anti-dUSP36 and anti-Fibrillarin antibodies. Images are shown as separate grayscale channels and as merged images. Blue: DAPI. Green: anti-dUSP36. Red: anti-Fibrillarin.

Figure 2

Growth phenotype of *dUsp36*^{C181S} mutants. *Drosophila* females (A) and wings (C) of the indicated genotype. Quantifications and statistical analyses of their weight (B) and wing area (D). GFP-positive clones of larval fat body cells homozygous for the indicated *dUsp36* allele (E). Quantifications of the relative cell size, expressed as the ratio between the area of a GFP+ cell and the mean area of neighbouring GFP- cells (F). Genotype: *hsFLP*/+; *CgGal4, UAS-GFP*/+; *FRT2A dUsp36*^{x}/*FRT2A TubGal80*. **** and *** indicate statistical significance with $P < 0.001$ and $P < 0.01$, respectively, as determined by one-way ANOVA.

Figure 3

Phenotypic effects of dMYC levels increase and decrease in *dUsp36* catalytic mutants. (A) Quantifications and statistical analyses of female fly weight for the indicated genotypes. "*Tg dMyc*" indicates the presence at the homozygous state of a transgene expressing a GFP-tagged version of dMYC within its genomic environment. (B) Histograms showing the observed frequency of males of the indicated genotypes in the progeny resulting from the following crosses: *dUsp36*^{CTL}/*TM6b* x *dUsp36*$^{\Delta 43}$/*TM6b*, *dUsp36*$^{C181S-1}$/*TM6b* x *dUsp36*$^{C181S-2}$/*TM6b*, *dMyc*^{P0}/*FM7c*; *dUsp36*^{CTL}/*TM6b* x *dUsp36*$^{\Delta 43}$/*TM6b*, and *dMyc*^{P0}/*FM7c*; *dUsp36*$^{C181S-1}$/*TM6b* x *dUsp36*$^{C181S-2}$/*TM6b*, respectively. (C, D) Quantifications and statistical analyses of wing areas of control and catalytic mutant flies expressing the wing-specific Gal4 driver *nubGal4*, either alone or in combination with RNAi transgenes targeting *dMyc* or *ago*. ****

and *** indicate statistical significance with P < 0.001 and P < 0.01, respectively, as determined by one-way ANOVA (A, C), chi-square test (B), and two-way ANOVA (D).

Figure 4

Fertility defects in *dUsp36* catalytic mutants. Quantifications and statistical analyses of the number of offspring produced by individual females (A) and males (B) of the indicated genotypes. (C) Testis stained with anti-dUSP36. The seminal vesicle is outlined. Blue: DAPI. Green: anti-dUSP36 antibody. (D) Quantifications and statistical analyses of the area of the seminal vesicle (S.V.). **** and *** indicate statistical significance with P < 0.001 and P < 0.01, respectively, as determined by one-way ANOVA."**

Figure S1

Generation of *dUsp36* catalytic mutants by CRISPR/Cas9 mutagenesis. (A) Schematic representation of the *dUsp36* locus with the three known isoforms. The position of the codon specifying the cysteine residue at position 181 is indicated as well as the gRNA (red triangle). WT: wild-type *dUsp36* sequence showing the targeted cysteine (in cyan), the sequence targeted by the gRNA (underlined in black) and the PAM (underlined in red). ssDNA: part of the ssODN sequence with the G-to-C transversion responsible for the C181S mutation and the silent mutations introduced for screening purposes (creation of a Pst1 restriction site and mutation of the PAM and of the gRNA to avoid re-cleaving of an edited chromosome). (B) Agarose gel showing that PCR products amplified from the $dUsp36^{CTL}$, $dUsp36^{C181S-1}$ and $dUsp36^{C181S-2}$ alleles display a Pst1 restriction site which is absent of the wild-type allele. (D) Chromatograms showing the sequences obtained from the two independent $dUsp36^{C181S}$ alleles, as well as from the control allele, $dUsp36^{CTL}$, which contains all the silent mutations introduced for screening purposes but not the G-to-C transversion responsible for the C181S mutation.

Figure S2

Rescue of the lethality of *dUsp36* null mutants by the ubiquitous expression of the double mutant $dUSP36^{C181S,\ H439D}$ protein.

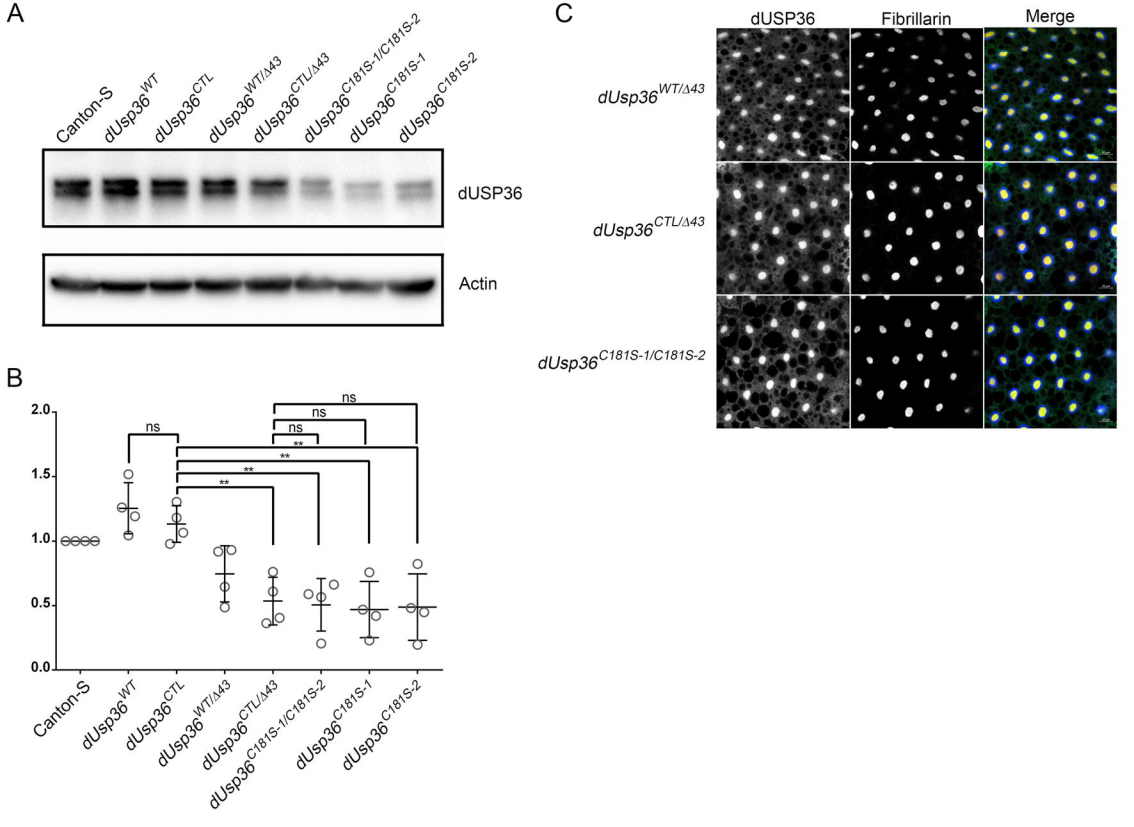
A
Canton-S
dUsp36WT
dUsp36CTL
dUsp36WT/Δ43
dUsp36CTL/Δ43
dUsp36C181S-1/C181S-2
dUsp36C181S-1
dUsp36C181S-2
dUSP36
Actin
B
2.0
1.5
1.0
0.5
0.0
ns
ns
ns
ns
**
**
**
**
Canton-S
dUsp36WT
dUsp36CTL
dUsp36WT/Δ43
dUsp36CTL/Δ43
dUsp36C181S-1/C181S-2
dUsp36C181S-1
dUsp36C181S-2
C
dUSP36
Fibrillarin
Merge
dUsp36WT/Δ43
dUsp36CTL/Δ43
dUsp36C181S-1/C181S-2

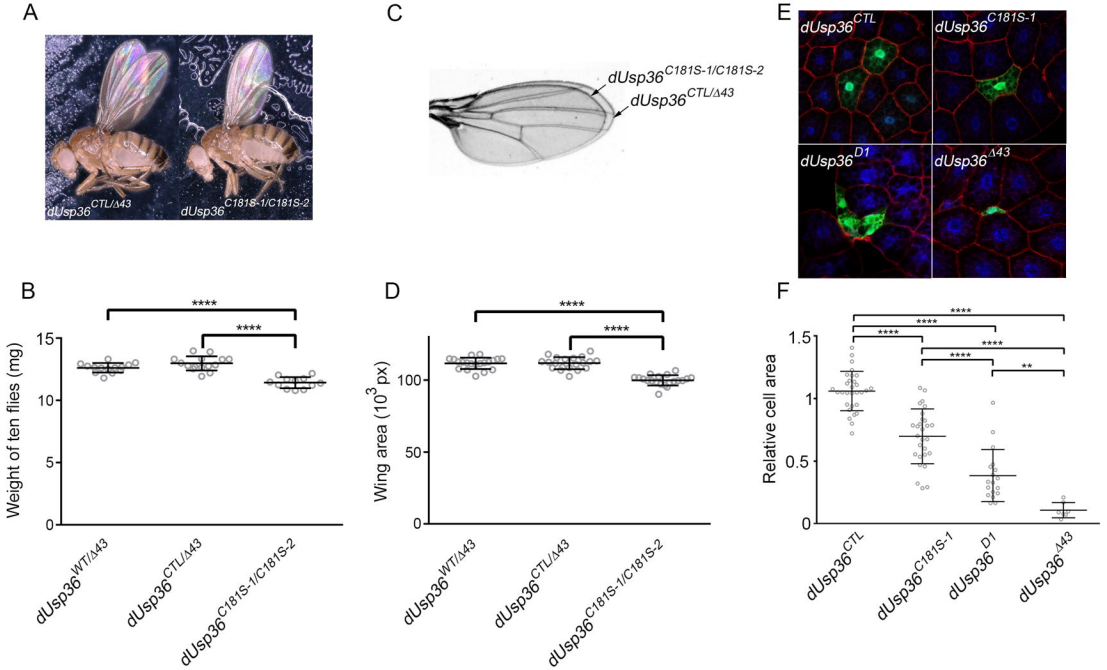
A
dUsp36CTL/Δ43
dUsp36C181S-1/C181S-2
C
dUsp36C181S-1/C181S-2
dUsp36CTL/Δ43
E
dUsp36CTL
dUsp36C181S-1
dUsp36D1
dUsp36Δ43
B
Weight of ten flies (mg)
15
10
5
0
****
****
dUsp36WT/Δ43
dUsp36CTL/Δ43
dUsp36C181S-1/C181S-2
D
Wing area (10^3 px)
100
50
0
****
****
dUsp36WT/Δ43
dUsp36CTL/Δ43
dUsp36C181S-1/C181S-2
F
Relative cell area
1.5
1
0.5
0
****
****
****
****
****
**
dUsp36CTL
dUsp36C181S-1
dUsp36D1
dUsp36Δ43

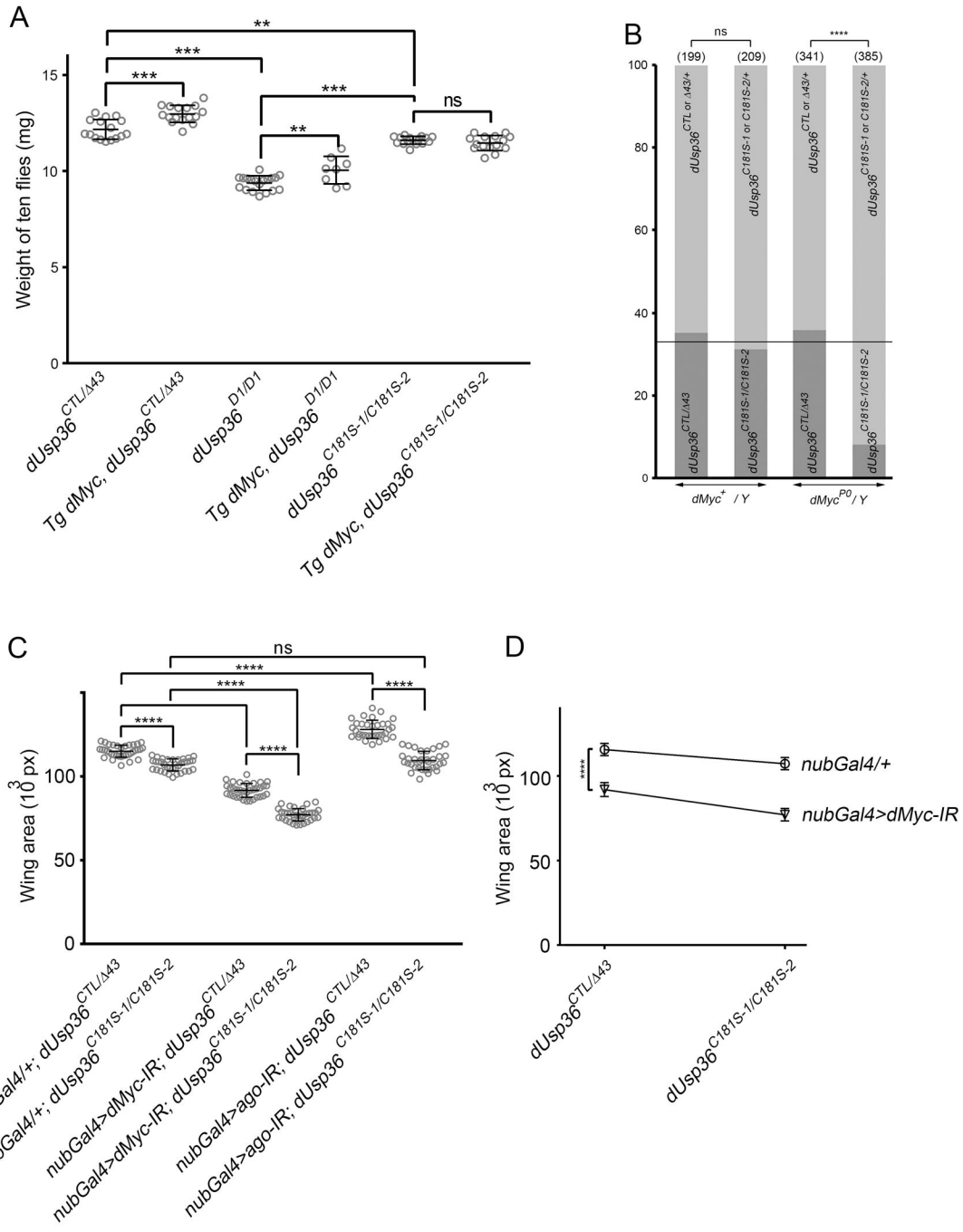
A
Weight of ten flies (mg)
0
5
10
15
**
***
***
***
**
ns
dUsp36CTL/Δ43
Tg dMyc, dUsp36CTL/Δ43
dUsp36D1/D1
Tg dMyc, dUsp36D1/D1
dUsp36C181S-1/C181S-2
Tg dMyc, dUsp36C181S-1/C181S-2
B
ns
****
(199)
(209)
(341)
(385)
100
80
60
40
20
0
dUsp36CTL or Δ43/+
dUsp36C181S-1 or C181S-2/+
dUsp36CTL/Δ43
dUsp36C181S-1/C181S-2
dMyc+ / Y
dMycP0 / Y
C
Wing area (10^3 px)
0
50
100
ns
****
****
****
****
****
nubGal4/+; dUsp36CTL/Δ43
nubGal4/+; dUsp36C181S-1/C181S-2
nubGal4>dMyc-IR; dUsp36CTL/Δ43
nubGal4>dMyc-IR; dUsp36C181S-1/C181S-2
nubGal4>ago-IR; dUsp36CTL/Δ43
nubGal4>ago-IR; dUsp36C181S-1/C181S-2
D
Wing area (10^3 px)
0
50
100
****
nubGal4/+
nubGal4>dMyc-IR
dUsp36CTL/Δ43
dUsp36C181S-1/C181S-2

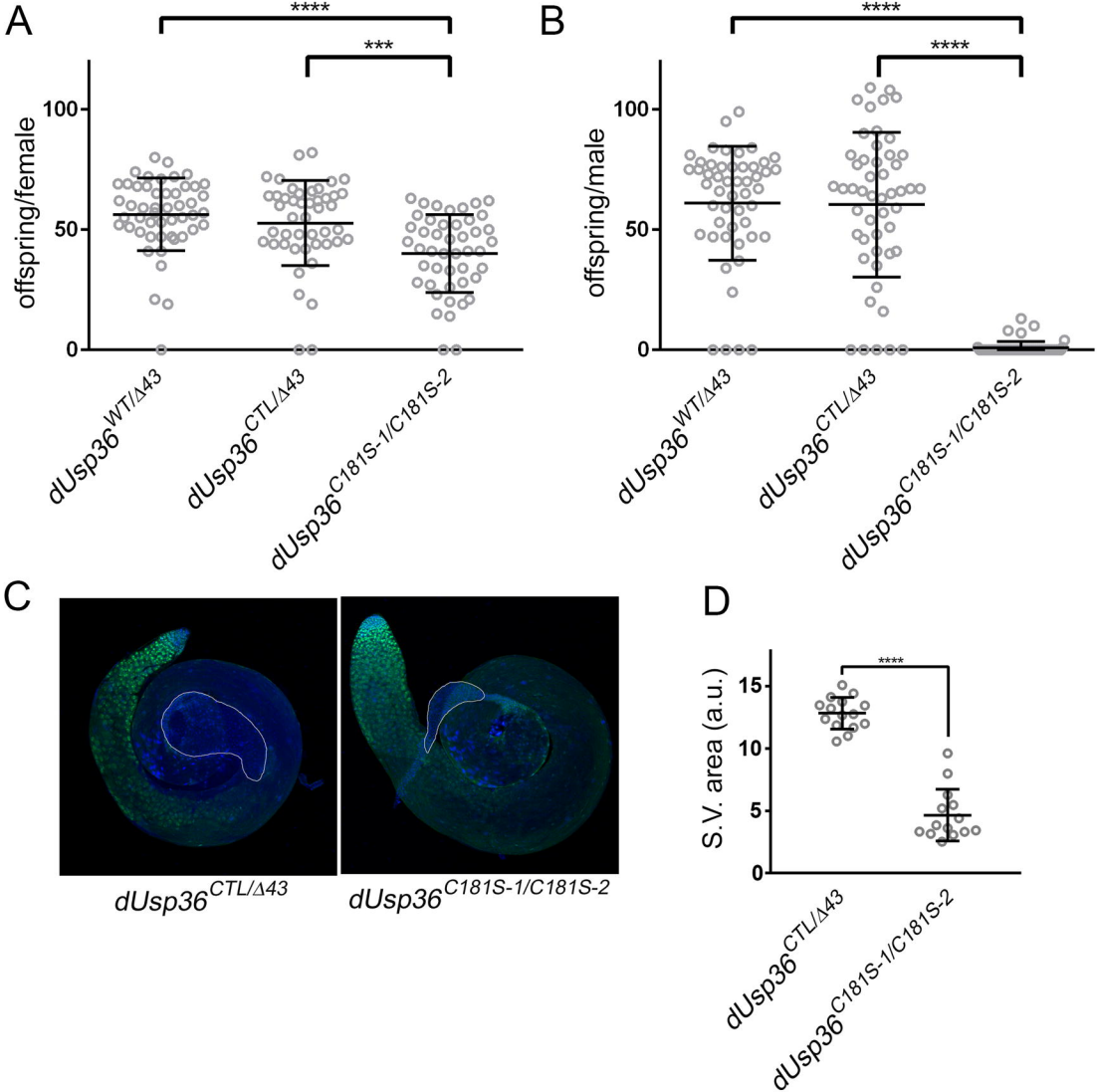
A
****
***
offspring/female
100
50
0
dUsp36WT/Δ43
dUsp36CTL/Δ43
dUsp36C181S-1/C181S-2
B
****
****
offspring/male
100
50
0
dUsp36WT/Δ43
dUsp36CTL/Δ43
dUsp36C181S-1/C181S-2
C
dUsp36CTL/Δ43
dUsp36C181S-1/C181S-2
D
****
S.V. area (a.u.)
15
10
5
0
dUsp36CTL/Δ43
dUsp36C181S-1/C181S-2